Photocounting Array Receivers for Optical Communication Through the Lognormal Atmospheric Channel. 1: Optimum and Suboptimum Receiver Structures

M. C. Teich and S. Rosenberg

The structure of the optimum direct detection array receiver is obtained for a system consisting of an amplitude-stabilized optical source, a lognormal channel, and a bank of photocounting detectors. Additive independent background radiation and detector dark current are taken into account. Both orthogonal and nonorthogonal M-ary signaling formats are considered. Attention is given to detection intervals small in comparison with the correlation time of the atmospherically induced fluctuations. A saddlepoint integration provides an excellent approximation to the optimum processor, resulting in a considerably simplified structure. Suboptimum aperture integration and *maximum a posteriori* (MAP) receivers are also considered. The performance of these receiver structures and their relative merits are presented in related papers (Parts 2 and 3).

I. Introduction

In a previous paper the statistical description of the output signal from an array of photoelectron counters was developed.[1] The incident radiation was considered to pass through the lognormal atmospheric channel and to contain additive background radiation as well as coherent signal. Probability distributions for the photoelectron counts, both in the presence of noise plus faded signal, and in the presence of noise alone, were obtained. Exact expressions for the first-, second-, and third-order photocounting cumulants for lognormally modulated mixtures of coherent and chaotic radiation were also calculated.[2] In this paper, these results are used to examine the problem of optimum detection. Only clear-air turbulence[3,4] is considered; atmospheric scattering and absorption are taken into account only insofar as they may uniformly reduce the irradiance at the receiver. The performance of wide field-of-view receivers employing optical scattering links has been considered elsewhere[5] and will not be dealt with here.

The detected process is assumed to be the output signal from an array of photodetectors, which direct detect the incident radiation. For detectors with positive gain (e.g., photomultipliers) the thermal noise introduced at the detector can generally be neglected in comparison with the quantum, or shot noise, of the detected signal and background radiation.[6]

The radiation arriving at the receiver is considered to have been modified by an effective multiplicative random process that characterizes the effects of the turbulent atmosphere.[7] Furthermore, for signal bandwidths of interest, the fading may be assumed constant over the detection interval T. Thus $T \ll \tau_a$, with τ_a the characteristic fluctuation time for the atmospherically induced fading. This is justified by the relatively long typical coherence time for the atmosphere ($\sim$1 msec). The fading statistics for the irradiance are taken to be lognormal in light of most experimental evidence to date.[8-11] Added to the faded signal radiation is (signal-independent) background noise modeled by a white zero-mean complex Gaussian process that is stationary in time and space.[7] For most practical receivers, the effect of the background radiation on the counting process is equivalent to the addition of independent noise photocounts at each detector in the array.[1] These counts are Poisson distributed with constant mean, proportional to the background noise power density. The background noise takes into account various thermal radiation sources such as scattered solar radiation, direct solar radiation, moonlight, blackbody radiation, etc. A block diagram of this communication system is indicated in Fig. 1.

The direct detection photocounting distributions for lognormally faded laser radiation have been eval-

M. C. Teich is with the Department of Electrical Engineering & Computer Science, Columbia University, New York, New York 10027; S. Rosenberg is with Bell Laboratories, Whippany, New Jersey 07981.

Received 26 January 1973.

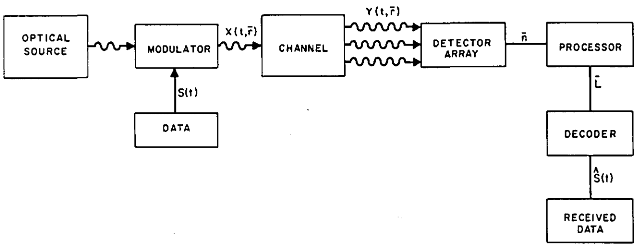

Fig. 1. Block diagram for the direct detection array photocounting communications system. The channel under consideration is the clear-air turbulent atmosphere. A bar over a given quantity symbolizes that it is a vector.

uated by Diament and Teich[12,13] and by others[14–16] for a single detector and by Teich and Rosenberg[1,2] for an array of detectors. The effects of turbulence on optical radar and on the binary communication channel for *heterodyne* detection were examined by Fried and Schmeltzer,[17] and by Heidbreder and Mitchell.[18] Kennedy and Hoversten[7] presented the structures and error bounds for M-ary orthogonal signaling and heterodyne detection for fading on D independent paths. Halme[19] extended Kennedy and Hoversten's results to arbitrary correlation and investigated various representations of the detected field in the aperture. One of Halme's conclusions is that only the sampling representation of the field in the aperture is amenable to analysis; this is the representation to be used here as well.

For *direct* detection optical communications in the presence of lognormal fading, few detailed results are available. Peters and Arguello[20] have obtained the error probabilities for a polarization modulation system, using an ideal amplitude-stabilized source with a single detector per channel, in the presence of lognormal fading. These authors do not include background radiation and dark current, however. Solimeno *et al.*[21] presented binary error probabilities for direct detection in the presence of lognormal fading at a single detector. The case they consider, however, is one in which the fluctuations of the background radiation are discernible. That is, the counting time T was taken to be significantly smaller than the background radiation coherence time τ_c, and thus the counting distribution in the absence of signal is Bose-Einstein, instead of Poisson, as considered here. In view of the fractional bandwidth of available optical interference filters, the coherence time of background radiation is generally $\lesssim 10^{-12}$ sec, and the assumption that the background statistics are resolved is unrealistic. Furthermore, the method given to obtain the error probabilities says nothing of the processing to be performed on the observed counts. Recently, Hoversten *et al.*[22] presented some results relating to the structure of optimum direct detection receivers for ideal laser sources, but the results they present assume independent fading at each detector in the array. Except for an error bound to a single-detector counting receiver, which is optimum for binary orthogonal equal-energy signals,[23] no quantitative performance results were presented. Explicit evaluation of error probabilities and information rates for a single-detector binary pulse-code modulation (BPCM) link, assuming a generalized laser source and lognormal fading, were recently presented by Yen *et al*,[24] however.

In this paper (Part 1) we obtain the optimum receiver structures, based on a minimum probability of error criterion, for lognormally faded amplitude-stabilized radiation with arbitrary fading correlation. This radiation is array detected in the presence of additive independent Poisson noise photocounts. Both orthogonal and nonorthogonal M-ary signaling formats are considered. In addition, we examine several suboptimal receiver structures.

In Part 2,[25] we obtain quantitative results for the performance of the structures presented in Part 1, as measured by the total probability of error per bit, for several binary signaling formats. In Part 3,[25] we derive a theoretical upper bound to the error probability for M-ary equal-energy, equiprobable orthogonal signals over D diversity paths, assuming flat independent fading.

II. Channel Model

Clear-air turbulence produces random fluctuations in the amplitude and phase of a transmitted optical wave, caused by the random variation of the optical index of refraction, in time and space, along a propagation path.[26] The resulting effects significantly degrade the transmitted wave, as measured by space-time fading, loss of coherence, and spreading of the beam. In this work, we do not specifically consider the effects of haze, smog, clouds, or other atmospheric conditions producing scattering and absorption effects. One result of these effects is a net decrease in the strength of the optical field at the detector. Thus by clear-air turbulence we mean only those effects produced by index of refraction variations. A thorough review of the current theory of atmospheric turbulence has been given by Lawrence and Strohbehn.[4]

In addition to the effects of the turbulent atmosphere, we include in our channel model the effects of background radiation as produced by various thermal sources such as the sun, sky, ambient earthlight, etc.[27] When the receiver field of view does not include the sun, most of the natural optical radiation for wavelengths below 3 μm is due to reflected or scattered solar radiation. For wavelengths above 3 μm the dominant source of background radiation is the thermal radiation of the earth whose spectral shape is approximately that of a blackbody at 280 K.

The background radiation is modeled as a white zero-mean complex Gaussian process whose components in the receiver aperture are independent and stationary in space and time. This latter assumption is valid for apertures larger than a few wavelengths and most signal bandwidths of interest. The background radiation is characterized by its spectral radiance N_λ which has the units W/m^2 sra μm of optical bandwidth. In our channel model, the effect of this background radiation is introduced as an additive, signal-independent noise process that produces photoelectrons at the mean rate N_B.[28] Furthermore, we need not consider the cross-mixing of signal and noise components, since for direct detection in a shot-noise limited regime, these terms are negligible.[28,29]

Based on the previous sections, we formulate the channel model as follows. A temporally modulated linearly polarized wave with complex envelope given by $X(t,\mathbf{r}) = S(t)e(t,\mathbf{r})$ is transmitted. The real field corresponding to this complex envelope is $\mathrm{Re}[X(t,\mathbf{r})\exp(-j2\pi\nu t)]$. Here $e(t,\mathbf{r})$ represents the complex analytic field representation for the source, and $S(t)$ represents the temporal modulation, which in later sections is assumed to be of digital format. After traversing the clear-air turbulent atmosphere, and neglecting the propagation time delay, the field is of the form $Y(t,\mathbf{r}) = \exp[\psi(t,\mathbf{r})]X(t,\mathbf{r}) + e_B(t,\mathbf{r})$, where $\psi(t,\mathbf{r})$ is a complex Gaussian process completely specified by its mean and covariance,[4] and where $e_B(t,\mathbf{r})$ is the complex envelope of the relevant polarization component of the background noise radiation discussed in the previous section. (The complex noise field generally consists of two orthogonal independent polarization components of equal mean power.) After appropriate spatial and temporal preprocessing to limit the noise (which is assumed not to change the field statistics), the field is sampled at an array of point detectors, each of which produces photoelectron counts as the observable. The channel model is thus the same as that formulated by Kennedy and Hoversten[7] for heterodyne detection, except that in our direct detection scheme we allow for partially correlated fading at the array. It should be mentioned at least in passing, however, that some deviations from this model can occur, especially at severe turbulence levels.[15,16]

III. Photoelectron Counting Distributions

Based on a first-order quantum-mechanical perturbation interaction, it can be shown that the probability of observing a photoelectron emitted from a photocathode is described by the well-known conditionally inhomogeneous Poisson process.[30] Thus, the probability of emitting n photoelectrons in a time interval $(t,t+T)$ is given by

$$p(n,t,T|W) = [W^n \exp(-W)]/n!. \tag{1}$$

Here the integrated intensity or rate parameter W is defined by

$$W \equiv \frac{\eta}{h\nu}\int_t^{t+T}\int_A |V(t',\mathbf{r})|^2 dt' dA, \tag{2}$$

where the detector quantum efficiency η is assumed to be constant over the bandwidth of the detected radiation. The quantity $h\nu$ is the photon energy, and $V(t',\mathbf{r})$ represents the analytic signal. However, if the radiation is of a stochastic nature, an additional average over the statistic of $V(t',\mathbf{r})$ is required in order to obtain the photoelectron counting distribution.

We further assume that the field maintains complete first-order spatial coherence over each detector surface, and thus the spatial integral merely produces a constant, representative of the detector area. With A_d the detector area and $\alpha \equiv \eta A_d/h\nu$, the joint photoelectron counting distribution for an array of detectors may be written as[1,31]

$$p(\mathbf{n},t,T) = \left\langle \prod_i \frac{W_i^{n_i}\exp(-W_i)}{n_i} \right\rangle_{\{W_i\}} \tag{3}$$

with

$$W_i = \int_t^{t+T} \alpha_i |V_i(t')|^2 dt'. \tag{4}$$

The angular brackets indicate an ensemble average over the statistics of $\{W_i\}$. Equation (3) is often referred to as Mandel's formula.[31] For simplicity, we further assume that the photodetector impulse response is ideal. That is, we assume that individual photoelectrons can be resolved.

Considering a radiation source that produces a Poisson counting process conditioned only on the fading, the integrated intensity for the ith detector, W_i, is given by

$$W_i = Z_i N_{Si} + N_B. \tag{5}$$

Here N_{Si} is the mean count due to the signal energy at the ith detector, Z_i is the normalized fading intensity, and N_B includes the contribution of background radiation as well as detector dark current, which can also be represented by an independent Poisson process.[32] The results derived here apply to an amplitude-stabilized laser operated well above threshold or to a source of arbitrary statistics provided that $T/\tau_c \gg 1$. Most thermal and laser sources used in optical communication systems are likely to fit in this category.

The conditional counting distribution for an array of D detectors is therefore given by

$$p(\mathbf{n}|\mathbf{Z}) = \prod_{i=1}^{D} \frac{(Z_i N_{Si} + N_B)^{n_i}\exp[-(Z_i N_{Si} + N_B)]}{n_i!}. \tag{6}$$

Averaging over the joint density for the normalized fading random variables $\{Z_i\}$, the counting distribution becomes[1]

$$p(\mathbf{n};\mathbf{N}_S;\Lambda) = \int_0^\infty p(\mathbf{n};\mathbf{N}_S|\mathbf{Z})p(\mathbf{Z})d\mathbf{Z}, \tag{7a}$$

where

$$p(\mathbf{Z}) = [(2\pi)^{D/2}|\Lambda|^{1/2}Z_1Z_2\ldots Z_D]^{-1}\exp\{-\tfrac{1}{2}\mathbf{X}^\dagger\Lambda^{-1}\mathbf{X}\}. \tag{7b}$$

The vector $\mathbf{X}$ has components given by

$$X_i = \ln Z_i + (\sigma_i^2/2), \quad i = 1,2,\ldots,D. \tag{8a}$$

Here the log-irradiance covariance matrix Λ contains elements given by

$$\Lambda_{ij} = C_{\ln I}(\mathbf{r}_i,\mathbf{r}_j), \quad i,j = 1,2,\ldots,D, \tag{8b}$$

where

$$\Lambda_{ii} = C_{\ln I}(\mathbf{r}_i,\mathbf{r}_i) = \sigma_i^2 \tag{8c}$$

is the log-irradiance variance. The vector $\mathbf{r}_i$ specifies the position of the ith detector.

We now apply the method of steepest descent,[1,12] but here with the relevant quantities defined as follows:

$$X_{i0} = \ln Z_{i0} + (\sigma_i^2/2), \tag{9a}$$

$$Q_i^{(1)}(n_i; Z_{i0}N_{Si}) = \frac{n_i Z_{i0} N_{Si}}{Z_{i0}N_{Si} + N_B} - Z_{i0}N_{Si}, \tag{9b}$$

$$Q_{ij}^{(2)}(n_i; Z_{i0}N_{Si}) = \left[\frac{n_i Z_{i0} N_{Si} N_B}{(Z_{i0}N_{Si} + N_B)^2} - Z_{i0}N_{Si}\right]\delta_{ij}, \tag{9c}$$

and

$$\mathbf{B}^* = \begin{bmatrix} Q_{11}^{(2)} & Q_{12}^{(2)} \cdots Q_{1D}^{(2)} \\ Q_{21}^{(2)} & Q_{22}^{(2)} \cdots & \cdot \\ \vdots & \vdots & \vdots \\ Q_{D1}^{(2)} & \cdots\cdots & Q_{DD}^{(2)} \end{bmatrix} - \Lambda^{-1}. \tag{9d}$$

The subscript 0 represents the stationary point. The counting distribution then takes the explicit form

$$p(\mathbf{n}; \mathbf{N}_S; \Lambda) = \frac{\left(\prod_{i=1}^{D} \frac{(Z_{i0}N_{Si} + N_B)^{n_i} \exp[-(Z_{i0}N_{Si} + N_B)]}{n_i!}\right) \exp\{-\frac{1}{2}\mathbf{X}_0^\dagger \Lambda^{-1} \mathbf{X}_0\}}{|\Lambda|^{1/2}|-\mathbf{B}^*|^{1/2}}, \tag{10}$$

where the stationary point $\mathbf{Z}_0$ is obtained from the equation

$$\mathbf{Q}^{(1)}(\mathbf{n}; \mathbf{Z}\mathbf{N}_S) - \Lambda^{-1}\mathbf{X} = 0. \tag{11}$$

The counting distribution given by Eq. (10) was previously evaluated, and graphically presented for the case $D = 2$ as a function of the various parameters of interest.[1]

The noise counting distribution is given by

$$p(\mathbf{n}; N_B) = \prod_{i=1}^{D} \frac{N_B^{n_i} \exp(-N_B)}{n_i!}, \tag{12}$$

where it is assumed that the mean noise count at each detector in the array is N_B. In the following section we use these results to obtain the optimum receiver structures based on a minimum probability of error constraint.

IV. Optimum Receiver Structures

First we consider the binary signaling problem; we must decide by some appropriate scheme whether the detected photoelectron counts are a result of a signal-plus-noise being present or a result of noise alone. This is referred to as the binary hypothesis testing problem. Let H_1 be the hypothesis that a signal is present and H_0 the hypothesis that it is not. It can then be shown that based on a Bayes criterion, the quantity that minimizes the average risk, and in this case the total probability of error, is obtained from the likelihood ratio test.[33] This test specifies that either H_1 or H_0 be chosen depending on the result of the inequality for the likelihood ratio $\underline{\Lambda}(\mathbf{n})$:

$$\underline{\Lambda}(\mathbf{n}) \equiv \frac{p_1(\mathbf{n})}{p_0(\mathbf{n})} \underset{H_0}{\overset{H_1}{\gtrless}} \frac{1-\pi_1}{\pi_1}, \tag{13}$$

where $p_1(\mathbf{n})$ is the density of $\mathbf{n}$ under H_1, and $p_0(\mathbf{n})$ is the density of $\mathbf{n}$ under H_0. Here π_1 is the *a priori* probability that a signal is present, while $\pi_0 = 1 - \pi_1$ is the *a priori* probability that it is not.

Equivalently, since the logarithm is a monotonic function, the logarithmic likelihood ratio $L(\mathbf{n})$ is given by

$$L(\mathbf{n}) \equiv \ln\underline{\Lambda}(\mathbf{n}) \underset{H_0}{\overset{H_1}{\gtrless}} \ln\left(\frac{1-\pi_1}{\pi_1}\right). \tag{14}$$

Since we are concerned primarily with digital communication, we assume for simplicity that $\pi_1 = \frac{1}{2}$. That is, the hypotheses present and not present are taken to be equally likely.

The likelihood ratio then reduces to the simple form

$$\underline{\Lambda}(\mathbf{n}) \underset{H_0}{\overset{H_1}{\gtrless}} 1, \tag{15}$$

and the likelihood function becomes

$$L(\mathbf{n}) \underset{H_0}{\overset{H_1}{\gtrless}} 0. \tag{16}$$

The log-likelihood ratio or likelihood function is usually the quantity that reveals the receiver structure. That is, it tells us how to process the observed data $\mathbf{n}$ in order to decide whether to choose H_1 or H_0.

Similarly it can be shown that for M equally likely hypotheses, the test that corresponds to minimizing the total probability of error is the maximum likelihood test, where one chooses the kth hypothesis if $L_k \geq L_j$ for $j = 1, \ldots, M$. That is, we choose the likelihood function that is largest as corresponding to the correct hypothesis. If likelihood draws occur, any random choice can be made without affecting the total probability of error.[33]

A. Optimum Processor

We begin this section by considering the simple binary detection problem where there either is, or is not, a signal present.

From Eqs. (6), (7a), (12), and (13), we obtain

$$\underline{\Lambda}(\mathbf{n}) = \frac{\int_0^\infty \cdots \int_0^\infty \left(\prod_{i=1}^{D} (Z_i N_{Si} + N_B)^{n_i} \exp[-(Z_i N_{Si} + N_B)] \right) p(Z_1, Z_2, \ldots, Z_D) dZ_1 \ldots dZ_D}{\prod_{i=1}^{D} N_B{}^{n_i} \exp(-N_B)}, \quad (17)$$

where $p(\mathbf{Z})$ is given by Eq. (7b). The likelihood function is then

$$L(\mathbf{n}) = \ln\left[\int_0^\infty \cdots \int_0^\infty \left[\prod_{i=1}^{D} \left(\frac{Z_i N_{Si}}{N_B} + 1\right)^{n_i} \times \exp(-Z_i N_{Si})\right] p(\mathbf{Z}) d\mathbf{Z}\right]. \quad (18)$$

The density of the lognormal variates $\{Z_i\}$ is in general that of correlated variables, and the receiver structure is rather complex due to the highly nonlinear nature of the functions involved. The saddle-point method, as used in Ref. 1, will allow us to obtain a tractable receiver structure that provides an excellent approximation to the performance of the optimum structure specified by Eq. (18).

The structure of Eq. (18) can be further simplified if we allow $N_{Si} = N_S$ independent of i, implying that the same mean signal energy is present at each detector. It has already been assumed that $N_{Bi} = N_B$. Furthermore, if the fades at all the detectors are statistically independent and of equal strength ($\sigma_i = \sigma_j$), the optimum receiver structure is given by

$$L = \ln \prod_{i=1}^{D} \left[\int_0^\infty \left(\frac{Z N_S}{N_B} + 1\right)^{n_i} \exp(-Z N_S) p(Z) dZ \right], \quad (19)$$

where $p(Z)$ is the one-dimensional lognormal distribution.[12,13] This structure corresponds to a nonlinear weighting of the counts from each detector, before combining.

For M equally likely signals, the optimum receiver forms the structure of Eq. (18) with N_{Si} replaced by N_{Sk}, where again i refers to the ith detector and k refers to the kth waveform, for each of the possible M waveforms. For equal-energy orthogonal signals, L_k is given by Eq. (18) with n_i replaced by n_{ik} and N_{Si} by N_S.

If we allow $D = 1$, the test corresponding to $L_k \geq L_j$ for equal-energy orthogonal signals is

$$\int_0^\infty \left(\frac{Z N_S}{N_B} + 1\right)^{n_k} \exp(-Z N_S) p(Z) dZ \geq \int_0^\infty \left(\frac{Z N_S}{N_B} + 1\right)^{n_j} \exp(-Z N_S) p(Z) dZ, \quad (20)$$

where n_k is the observed count assuming that the energy detected is associated with the kth signal of the M possible orthogonal signals. This is equivalent to testing whether $n_k \geq n_j$, since the functionals are monotonically increasing with n_k. Thus for M-ary equal-energy orthogonal waveforms and one detector, in the presence of turbulence, the optimum receiver is that of unweighted photoelectron counting, just as in the absence of turbulence. As will be shown in the next section, the approximate optimum receiver, based on the likelihood function saddle-point solution for this case, does not reduce to the counting receiver except for $D = 1$. It should be pointed out that the use of the instantaneous fade level Z in calculating the estimator can result in a fixed threshold that appears to be independent of Z.

B. Approximate Optimum Processor

In order to determine the processing implied by the likelihood functions given in the previous section, we resort to a saddle-point solution, as was done in obtaining the counting distribution. Applying this method[1] and assuming uniform average irradiance at the detector array, we obtain the following likelihood ratio:

$$\underline{\Lambda}(\mathbf{n}) = \left[\prod_{i=1}^{D} \left(\frac{Z_{i0} N_S}{N_B} + 1\right)^{n_i} \exp(-Z_{i0} N_S)\right] \times \frac{\exp\{-\frac{1}{2}\mathbf{X}_0{}^{\dagger}\Lambda^{-1}\mathbf{X}_0\}}{|\Lambda|^{1/2}|-\mathbf{B}^*|^{1/2}}. \quad (21)$$

The receiver structure is then given by

$$L = \left[\sum_{i=1}^{D} n_i \ln\left(\frac{Z_{i0} N_S}{N_B} + 1\right) - Z_{i0} N_S\right] - \tfrac{1}{2}\mathbf{X}_0{}^{\dagger}\Lambda^{-1}\mathbf{X}_0 - \tfrac{1}{2}\ln|\Lambda| - \tfrac{1}{2}\ln|-\mathbf{B}^*|, \quad (22)$$

for the binary case.

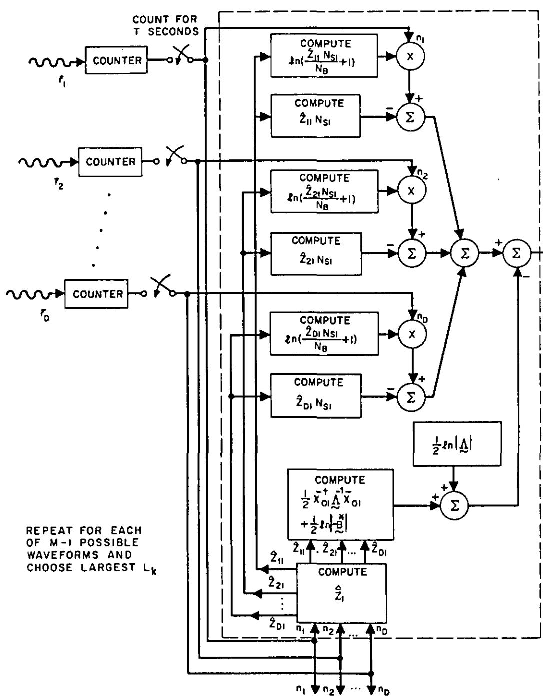

Fig. 2. Approximate optimum array receiver for partially correlated fading and M-ary signaling. $\hat{\mathbf{Z}}_k$ is the solution to the MAP estimator equation for the kth signal waveform, and $\mathbf{X}_{01}$ represents $\mathbf{X}_{0k}$. Uniform average illumination of the array is assumed so that N_{S1} represents N_{Sk} rather than N_{Si}.

The receiver thus performs weighted counting, where the weights now depend on the solution of the stationary equation, Eq. 11, and thus on the observed counts. Bias terms that depend on the covariance matrix of the fading, and on the matrix $\mathbf{B}^*$, must be subtracted. It is in these bias terms that the processor weights the counts optimally, deemphasizing those with strong fades about the mean signal count. If in addition a signal is present (in the binary case), the modal points $\{Z_{i0}\}$ form *maximum a posteriori* (MAP) estimates, $\{\hat{Z}_i\}$, of the fading at each detector in the array, as will be shown. We will later examine a suboptimum receiver that attempts to measure the fading on each signaling interval, and using that noisy estimate, processes the counts as if the fading were known.

For M-ary signals, the approximate optimum processor forms Eq. (22) for each of the possible M waveforms. This receiver is shown in Fig. 2, where $\mathbf{Z}_0$ is indicated by $\hat{\mathbf{Z}}$ for simplicity of notation.

A receiver structure similar to that obtained here, but for independent flat fading, has been given by Hoversten *et al.*[22] The receiver structure solutions given there are based on the Bar-David formulation of the Poisson process, in terms of the time occurrences of the individual photoelectron pulses, rather than on the total number of pulses observed during the detection interval $(0,T)$.[34] The Bar-David formulation is more useful in radar and waveform estimation, where time occurrences of events are important. The solution based on the Mandel formula lends itself more readily to the evaluation of receiver performance, however, and has been used for that reason. It should be noted that in contrast to previous results, the strucuture specified here is more general in that it accounts for the possibility of correlated fading.

C. Independent Fading Samples

The structure of Eq. (22) can be further simplified if the fading at each detector is independent of the fading at every other. In that case the covariance matrix Λ and the matrix $\mathbf{B}^*$ are diagonal, and the receiver structure reduces to

$$L = \sum_{i=1}^{D}\Bigg[n_i \ln\left(\frac{Z_{i0}N_S}{N_B} + 1\right) - Z_{i0}N_S - \frac{[\ln(Z_{i0}) + (\sigma_i^2/2)]^2}{2\sigma_i^2} - \tfrac{1}{2}\ln\left\{\sigma_i^2\left[\frac{-n_i Z_{i0}N_S N_B}{(Z_{i0}N_S + N_B)^2} + Z_{i0}N_S\right] + 1\right\}\Bigg], \quad (23)$$

where the $\{Z_{i0}\}$ are now obtained from an uncoupled set of stationary equations given by

$$\frac{n_i Z_{i0}N_S}{Z_{i0}N_S + N_B} - Z_{i0}N_S - \frac{[\ln(Z_{i0}) + (\sigma_i^2/2)]}{\sigma_i^2} = 0 \quad \text{for } i = 1,2,\ldots,D. \quad (24)$$

Equations (23) and (24) are similar to those given by J. N. Bucknam and first published by Hoversten *et al.*[22] (The expressions given there do not appear to be correct, however.) For M-ary signaling, we form M such functionals, where now $N_S \to N_{Sk}$, and choose the largest. The structure for this receiver is given in Fig. 3.

The approximate optimum processors discussed to this point provide an excellent approximation to the exact optimum processors; their performance will be evaluated and presented in Part 2 for binary pulse-code modulation (BPCM), binary polarization modulation (BPOLM), and binary pulse-interval modulation (BPIM).[25] In Part 3, we consider M-ary equal-energy equiprobable orthogonal signaling with flat independent fading.[25] We now turn to some suboptimum receiver structures that are often considerably easier to implement.

V. Suboptimum Receiver Structures

It is of interest to investigate some suboptimum receiver structures in order to evaluate the tradeoff between complexity in processing and degradation of performance. In particular, we investigate structures for the aperture integration and MAP receivers.

A. Aperture Integration Receiver

The aperture integration receiver consists of a single large detector encompassing the area covered by the array of D detectors considered in previous sections. The detector area is assumed to encompass D independent coherence areas of the faded signal, plus independent additive background noise radiation. The integrated intensity W is therefore given by

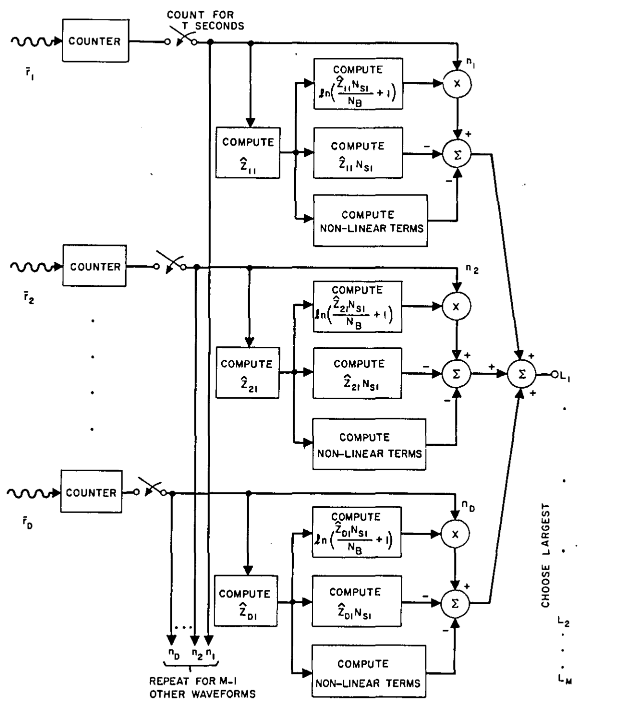

Fig. 3. Approximate optimum array receiver for independent fading and M-ary signaling. In this case the $\hat{Z}_{ik}$ are obtained from an uncoupled set of stationary equations. The quantity N_{S1} represents N_{Sk}, as in Fig. 2, indicating that uniform average illumination is assumed at the detector aperture.

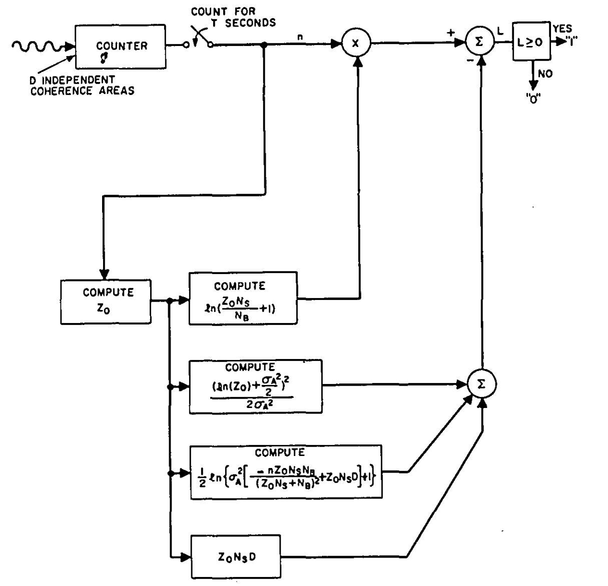

Fig. 4. Approximate optimum aperture integration receiver for BPCM with lognormal fading.

$$W = ZDN_S + DN_B,$$

where $D \approx A_d/A_c$, the number of independent coherence areas in the detector aperture. The random variable Z is now given by

$$Z = \frac{1}{A_d}\int_{A_d} Z(\mathbf{r})d\mathbf{r}. \tag{26a}$$

Based on studies of the statistics of this quantity,[35,36] it is clear that Z is well approximated by a lognormal random variable for large D. Furthermore, it can be shown that $X = \ln Z$ is Gaussian with mean $-\sigma_A{}^2/2$ and variance

$$\sigma_A{}^2 = \ln\left[\frac{e^{\sigma^2} - 1}{D} + 1\right], \tag{26b}$$

from which the variance of Z is $[\exp(\sigma^2)-1]/D$. This expression shows the effect of aperture averaging of the scintillations.[37] It should be noted that the expression for the variance is exact; the approximation rests on the assumption that Z is lognormal.

Experimental evidence, however, indicates that the maximum aperture averaging observed is that which reduces the variance of Z to a minimum value of about 10% of the unaveraged value.[38] Thus there appears to be a limit on the performance of an aperture integration receiver, and further improvement can only be obtained by resorting to detector arrays.

Based on the foregoing assumptions and analysis, the receiver structure is given by Eq. (23) with the summation on i dropped, $\sigma_i{}^2$ replaced with $\sigma_A{}^2$, and N_S and N_B replaced by DN_S and DN_B, respectively. The receiver then decides that a signal is present if $L \geq 0$ and that no signal is present if $L < 0$. As can be seen from the equation, the receiver weighs the counts in a nonlinear fashion before combining, as previously, but the over-all receiver structure is considerably simpler than for the array, as illustrated in Fig. 4 (compare with Fig. 3).

For M-ary signaling, the optimum aperture integration receiver forms the quantities L_k and chooses the signal corresponding to the largest. For equal-energy orthogonal signals, however, the modal points Z_{0k} are dependent on n_k. The weights are thus data dependent and are different for different values of n_k. Thus, the processing does not *appear* to reduce to unweighted photoelectron counting. Nevertheless, since Z_0 can be shown to be a monotonically increasing function of n, with all other parameters constant, then for equal-energy orthogonal signals the operation performed by the approximate optimum receiver is equivalent to comparing n_k with n_j, that is, to unweighted counting (see Fig. 5) as shown earlier.

B. MAP Receiver

Another possible scheme for reducing the complexity of the receiver is one in which a noisy estimate is made of the fading, under the assumption that a signal is present, and then used in the maximum likelihood receiver as if the fading were exactly known. The noisy estimate is obtained from the *maximum a posteriori* estimate of the fading Z. This is found from the MAP equation[33]

$$(\partial/\partial\mathbf{Z})p(\mathbf{Z}|\mathbf{n}) = (\partial/\partial\mathbf{Z})\{p(\mathbf{n}|\mathbf{Z})p(\mathbf{Z})/p(\mathbf{n})\} = 0, \tag{27}$$

where $p(\mathbf{Z}|\mathbf{n})$ is the *a posteriori* density of the fading, given that the photoelectron counts $\mathbf{n}$ have been detected. The quantity $p(\mathbf{n}|\mathbf{Z})$ is the conditional density of $\mathbf{n}$ given $\mathbf{Z}$. However, since $p(\mathbf{n})$ is independent of $\mathbf{Z}$, we must evaluate $(\partial/\partial\mathbf{Z})\{p(\mathbf{n}|\mathbf{Z})p(\mathbf{Z})\}$ or equivalently $(\partial/\partial\mathbf{Z})\{\ln p(\mathbf{n}|\mathbf{Z}) + \ln p(\mathbf{Z})\} = 0$. Since

$$p(\mathbf{n}|\mathbf{Z}) = \prod_{i=1}^{D}\frac{(Z_iN_S + N_B)^{n_i}\exp[-(Z_iN_S + N_B)]}{n_i!} \tag{28}$$

and $p(\mathbf{Z})$ is given in Eq. (7b), the MAP equation becomes

$$\mathbf{Q}^{(1)}(\mathbf{n},\mathbf{Z}) - \Lambda^{-1}\mathbf{X} = 0, \tag{29}$$

which is just the stationary equation, Eq. (11). The solution is now $\hat{\mathbf{Z}}$, and the likelihood ratio and likelihood function are thus given by

$$\underline{\Lambda}(\mathbf{n}) = \prod_{i=1}^{D}\left(\frac{\hat{Z}_iN_S}{N_B} + 1\right)^{n_i}\exp(-\hat{Z}_iN_S) \tag{30}$$

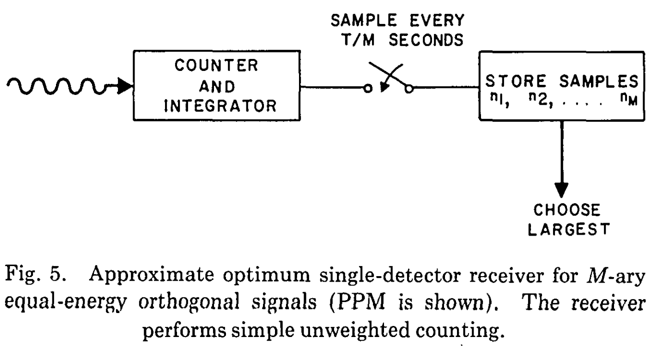

Fig. 5. Approximate optimum single-detector receiver for M-ary equal-energy orthogonal signals (PPM is shown). The receiver performs simple unweighted counting.

and

$$L(\mathbf{n}) = \sum_{i=1}^{D} n_i \ln\left(\frac{\hat{Z}_i N_S}{N_B} + 1\right) - \hat{Z}_i N_S, \qquad (31)$$

which take the form of weighted counts. As previously, for $L \geq 0$ we decide a signal is present. The receiver structure is thus considerably less complex than the approximate optimum array receiver, but at the cost of some performance. The precise performance of such a receiver is evaluated in Part 2.[25]

The results indicate that over several ranges of σ, N_S/N_B, and N_B, the MAP receiver performs almost as well as does the optimum receiver based on the saddle-point solution. It should be noted, however, that this receiver always estimates $\hat{\mathbf{Z}}$ whether a signal is present or not. Thus when a signal is absent, $\hat{\mathbf{Z}}$ is not a valid estimate and the performance is suboptimum, as is indicated by the error probability curves. However, if a signaling scheme is used such that there always is some signal present, analogous to a transmitted reference or pilot tone, the estimates will be valid, and the problem remains as to which one to choose or perhaps whether to long term average the estimates.

In all of the above receiver structures there is the implicit assumption that all other parameters, such as N_S, N_B, σ and Λ, are known exactly. Realistically these quantities must be obtained either before processing takes place or as part of the processor itself. However, the detected counts inherently contain all the information about the state of the channel, and thus by building the appropriate parameter estimators, analogous to the MAP estimator for the fading $\hat{\mathbf{Z}}$, these quantities can be measured.[22] Receivers that perform such channel measurement have been suggested in the past, but their performance for direct detection remains to be evaluated.

VI. Summary

We have obtained the optimum array receiver structures for lognormally faded amplitude-stabilized laser radiation, direct-detected in the presence of independent additive background radiation for arbitrarily correlated fading at the detector array. Receiver structures for both orthogonal and nonorthogonal M-ary signal formats were presented. The nature of the fading statistics resulted in complex receiver structures that were approximated by use of the saddle-point technique. Fortunately, the approximation mode used in obtaining these structures was found to be excellent, in the sense that the performance (bit error probability) is very close to that obtained using the exact receiver structures. In addition to the approximate optimum structures, several suboptimum structures were also investigated. The performance of these receiver structures and their relative merits are presented in accompanying papers (Parts 2 and 3).[25]

This work was supported in part by the National Science Foundation and is based on portions of a dissertation[39,40] submitted by S. Rosenberg to the Department of Electrical Engineering and Computer Science at Columbia University in partial fulfillment of the requirements for the degree of Doctor of Engineering Science.

References

1. M. C. Teich and S. Rosenberg, J. Opto-electron. **3**, 63 (1971): Note that Eq. (28) of this article should read $\mathbf{B} = \mathbf{Q}^{(2)} - \Lambda^{-1}$ and $|\mathbf{B}|^{1/2}$ should be replaced by $|-\mathbf{B}|^{1/2}$ throughout. All figures, results, conclusions, and other equations remain unchanged.
2. S. Rosenberg and M. C. Teich, J. Appl. Phys. **43**, 1256 (1972).
3. J. W. Strohbehn, Proc. IEEE **56**, 1301 (1968).
4. R. S. Lawrence and J. W. Strohbehn, Proc. IEEE **58**, 1523 (1970).
5. R. S. Kennedy, Proc. IEEE **58**, 1651 (1970).
6. W. K. Pratt, *Laser Communication Systems* (Wiley, New York, 1969), Chap. 9.
7. R. S. Kennedy and E. V. Hoversten, IEEE Trans. Inform. Theory **IT-14**, 716 (1968).
8. G. R. Ochs and R. S. Lawrence, J. Opt. Soc. Am. **59**, 226 (1969).
9. G. R. Ochs, R. R. Bergman, and J. R. Snyder, J. Opt. Soc. Am. **59**, 231 (1969).
10. P. H. Deitz and N. J. Wright, J. Opt. Soc. Am. **59**, 527 (1969).
11. G. E. Mevers, M. P. Keister, Jr., and D. L. Fried, J. Opt. Soc. Am. **59**, 491A (1969).
12. P. Diament and M. C. Teich, J. Opt. Soc. Am. **60**, 1489 (1970).
13. P. Diament and M. C. Teich, Appl. Opt. **10**, 1664 (1971).
14. J. Peřina and V. Peřinová, Czech. J. Phys. **B22**, 1085 (1972).
15. J. Peřina, V. Peřinová, and R. Horák, Czech. J. Phys. **B23**, to be published (1973); V. I. Tatarski, Zh. Eksp. Teor. Fiz. **61**, 1822 (1971) [Sov. Phys.-JETP **34**, 969 (1972)].
16. J. Peřina, V. Peřinová, M. C. Teich, and P. Diament, Phys. Rev. **A7**, 1732 (1973).
17. D. L. Fried and R. A. Schmeltzer, Appl. Opt. **6**, 1729 (1967).
18. G. R. Heidbreder and R. L. Mitchell, IEEE Trans. Aerosp. Electron. Syst. **AES-3**, 5 (1967).
19. S. J. Halme, "Efficient Optical Communications in a Turbulent Atmosphere," Technical Report 474, MIT Research Laboratory of Electronics (1970).
20. W. N. Peters and R. J. Arguello, IEEE J. Quantum Electron. **QE-3**, 532 (1967).
21. S. Solimeno, E. Corti, and B. Nicoletti, J. Opt. Soc. Am. **60**, 1245 (1970).
22. E. V. Hoversten, R. O. Harger, and S. J. Halme, Proc. IEEE **58**, 1626 (1970). See also E. V. Hoversten, "Optical Communication Theory," in *Laser Handbook,* F. T. Arecchi and E. O. Schulz-DuBois, Eds. (North-Holland, Amsterdam, 1972), p. 1805.
23. E. V. Hoversten and R. S. Kennedy, "Efficient Optical Communication within the Earth's Atmosphere," in *Opto-Electronics Signal Processing Techniques,* AGARD Conf. Proc. **50**, 5-1 (1970).
24. R. Y. Yen, P. Diament, and M. C. Teich, IEEE Trans. Inform. Theory **IT-18**, 302 (1972).
25. S. Rosenberg and M. C. Teich (Part 2), Appl. Opt. **12**, 2625 (1973) [following paper]; S. Rosenberg and M. C. Teich (Part 3), IEEE Trans. Inform. Theory **IT-19**, 807 (1973).
26. V. I. Tatarski, *Wave Propagation in a Turbulent Medium* (McGraw-Hill, New York, 1961).
27. N. S. Kopeika and J. Bordogna, Proc. IEEE **58**, 1571 (1970).
28. S. Karp and J. R. Clark, IEEE Trans. Inform. Theory **IT-16**, 672 (1970).
29. J. R. Kerr, Proc. IEEE **55**, 1686 (1967).
30. A. Papoulis, *Probability, Random Variables, and Stochastic*

Processes (McGraw-Hill, New York, 1965), p. 189.
31. L. Mandel, Proc. Phys. Soc. (London) 72, 1037 (1958).
32. M. Ross, *Laser Receivers* (Wiley, New York, 1966), Chap. 2.
33. H. L. Van Trees, *Detection, Estimation and Modulation Theory, Part I* (Wiley, New York, 1968).
34. I. Bar-David, IEEE Trans. Inform. Theory **IT-15**, 31 (1969).
35. B. K. Levitt, "Detector Statistics for Optical Communication through the Turbulent Atmosphere," Quarterly Progress Report 99, MIT Research Laboratory of Electronics (1970), p. 114.
36. R. L. Mitchell, J. Opt. Soc. Am. **58**, 1267 (1968).
37. D. L. Fried, J. Opt. Soc. Am. **57**, 169 (1967).
38. J. R. Kerr, P. J. Titterton, A. R. Kraemer, and C. R. Cooke, Proc. IEEE **58**, 1691 (1970).
39. For abstract of dissertation, see S. Rosenberg, IEEE Trans. Inform. Theory **IT-18**, 544 (1972).
40. A talk based on portions of this material was presented at the 1972 Annual Meeting of the Optical Society of America; for abstract, see S. Rosenberg, J. Opt. Soc. Am. **62**, 353A (1972).
